

UCRL-JC-131389

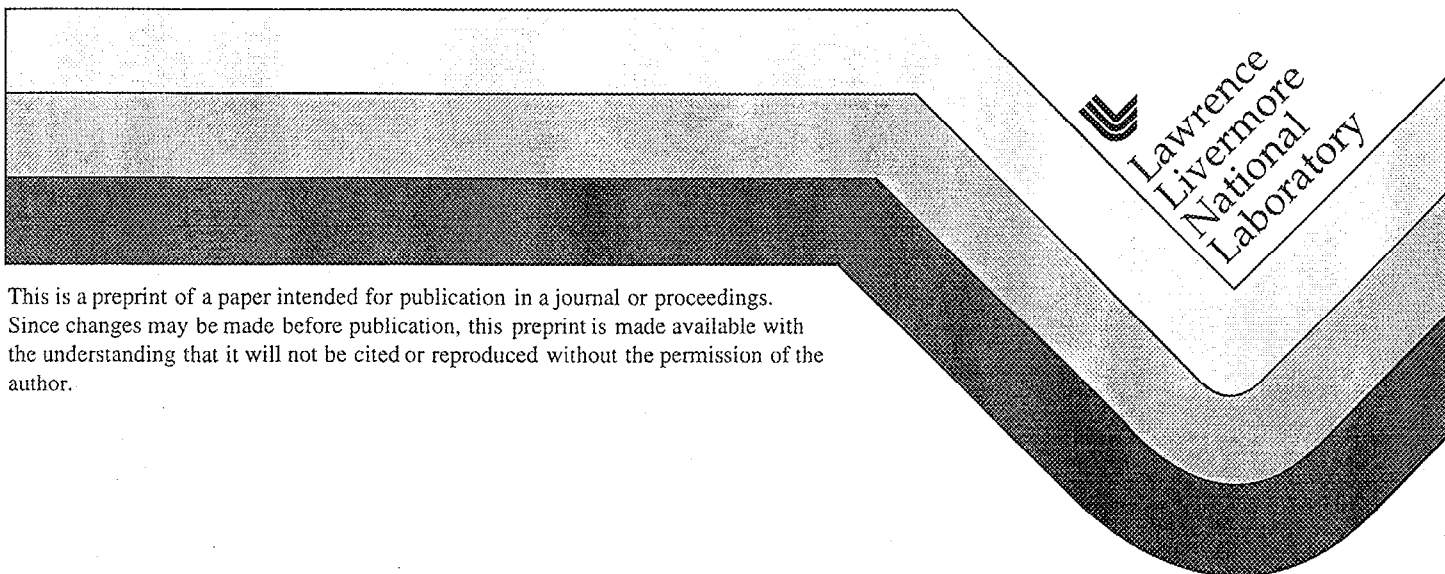
PREPRINT

# High Yield ICF Target Design for a Z-pinch Driven Hohlraum

J. H. Hammer, M. Tabak, S. C. Wilks, J. D. Lindl, D. S. Bailey,  
P. W. Rambo, A. Toor, G. B. Zimmerman, J. L. Porter, Jr.

This paper was prepared for submittal to the  
40th Annual Meeting of the Division of Plasma Physics  
New Orleans, LA  
November 16-21, 1998

November 13, 1998



This is a preprint of a paper intended for publication in a journal or proceedings.  
Since changes may be made before publication, this preprint is made available with  
the understanding that it will not be cited or reproduced without the permission of the  
author.

#### DISCLAIMER

This document was prepared as an account of work sponsored by an agency of the United States Government. Neither the United States Government nor the University of California nor any of their employees, makes any warranty, express or implied, or assumes any legal liability or responsibility for the accuracy, completeness, or usefulness of any information, apparatus, product, or process disclosed, or represents that its use would not infringe privately owned rights. Reference herein to any specific commercial product, process, or service by trade name, trademark, manufacturer, or otherwise, does not necessarily constitute or imply its endorsement, recommendation, or favoring by the United States Government or the University of California. The views and opinions of authors expressed herein do not necessarily state or reflect those of the United States Government or the University of California, and shall not be used for advertising or product endorsement purposes.

## High Yield ICF Target Design for a Z-pinch Driven Hohlraum

James H. Hammer, Max Tabak, Scott C. Wilks, John D. Lindl, David S. Bailey, Peter W.

Rambo, Arthur Toor and George B. Zimmerman

*Lawrence Livermore National Laboratory, Livermore, CA 94551*

John L. Porter, Jr.

*Sandia National Laboratories, Albuquerque, NM 87185-1191*

**Abstract:** We describe calculations for a high yield inertial fusion design, employing indirect drive with a double-ended z-pinch-driven hohlraum radiation source. A high current ( $\sim 60$  MA) accelerator implodes z-pinch within an enclosing hohlraum. Radial spoke arrays and shine shields isolate the capsule from the pinch plasma, magnetic field and direct x-ray shine. Our approach places minimal requirements on z-pinch uniformity and stability, usually problematic due to magneto-Rayleigh Taylor (MRT) instability. Large inhomogeneities of the pinch and spoke array may be present, but the hohlraum adequately smooths the radiation field at the capsule. Simultaneity and reproducibility of the pinch x-ray output to better than 7% are required, however, for good symmetry. Recent experiments suggest a pulse shaping technique, through implosion of a multi-shell z-pinch. X-ray bursts are calculated and observed to occur at each shell collision. A capsule absorbing 1 MJ of x-rays at a peak drive temperature of 210 eV is found to have adequate stability and to produce 400 MJ of yield. A larger capsule absorbs 2 MJ with a yield of 1200 MJ.

PACS 52.25.Nr, 52.50.Lp, 52.55.Ez, 52.58.Ns, 52.65.Kj

## I. INTRODUCTION

We consider an indirect drive inertial fusion design driven by z-pinch x-ray sources. The sources must drive the hohlraum to sufficient radiation temperature with an appropriate pulse shape and symmetry. The design, sketched in Fig. (1), is motivated by recent experiments on the Saturn and Z pulsed power accelerators, where high power x-ray production from imploding wire-array z-pinch has been achieved<sup>1</sup>. At 20 MA, the Z accelerator produces up to 2 MJ of x-rays with a peak power of 290 TW, and pulse widths as short as 4 ns. For our ICF targets, of order 16 MJ will be necessary, requiring a higher power driver. We must also find a means of providing the correct pulse shape, which entails heating the hohlraum to  $\sim 100$  eV for 20 ns before the main drive. Other recent experiments on Z<sup>2,3</sup> demonstrated a pulse-shaping technique: multiple shells. In these experiments, the imploding wire array impacted on foam shells or on an internal wire array, with a burst of x-ray emission at each impact. The concentric wire array experiment described in reference (3) was close to a hydrodynamic scale of the ICF pinch design, and produced timing and contrast similar to our calculations below. We discuss the scaling of pinch x-ray production and pulse shaping in greater detail in section II. The successful development of the z-pinch-driven hohlraum<sup>1,3</sup> is also important for our concept. A Z-pinch-driven hohlraum has an imploding pinch within a hohlraum with a narrow annular power feed. As for laser-heated hohlraums<sup>4</sup>, the radiation temperature in the hohlraum is set by a balance between emitted power and losses to the wall and power feed gap.

Adequate x-ray coupling and drive symmetry in the secondary hohlraum are also critical. Modeling of the coupled hohlraums, the current-return spokes separating the hohlraums, as well as static and time-dependent view factor calculations evaluating sym-

metry are discussed in section III. ICF capsule scaling<sup>4</sup> predicts ignition of capsules at 210 eV with adequate margin against Rayleigh-Taylor instability, if they are sized to absorb 1MJ or greater. This criterion is well matched to the hohlraum energetics for the ~60MA driver. We discuss the capsule design in section IV.

## II. Z-PINCH DYNAMICS AND PULSE SHAPING

The x-ray output for experiments on a variety of drivers has been found to scale with current,  $I$ , as  $I^2$ , consistent with most of the energy imparted by  $\mathbf{J} \times \mathbf{B}$  forces undergoing conversion to x-rays. At 60 MA, this scaling would give ~18 MJ of x-ray yield. Our concept employs a pinch geometry and driver approximately scaled from 2cm diameter implosions on Z. The current rise time and implosion velocity are comparable to the Z experiment, but at approximately 3 times the current. The shortest pulse width observed for 2cm diameter Z wire arrays is ~6 ns, while our ICF concept requires ~10 ns drive for the main pulse. The observed efficient conversion of magnetic energy to x-rays is consistent with 2D radiation magnetohydrodynamic calculations<sup>5,6</sup> but ab initio pinch calculations that accurately predict the pulse duration are not yet possible. The pulse duration and the energy release depend on instability growth. Instability levels depend on the pinch initiation which remains poorly understood. In 2D, axisymmetric calculations, the pinch is typically modeled as a shell with zone-to-zone random density perturbations of specified amplitude. The source of the density perturbation is presumed to be the breakdown and early-time instability of the wire array which may involve 3D effects not modeled. The most unstable modes of the imploding pinch are predicted to be axisymmetric magneto-Rayleigh Taylor instabilities, which can be included in the 2D calculations. Typically, a

perturbation level chosen in the range of 0.5 to a few percent with 50-100 micron zones can reproduce the experimental pulse width and give axial structure with mm wavelength scales as seen in framing images at stagnation. The pulse width, determined predominantly by the radial extent of bubble-spike structures, may vary by a factor of  $\sim 2$  as the perturbation is varied from 0.5% to 5%. The codes predict smaller radial extent of the x-ray "hot spots" than observed and 3D structure is also often evident at stagnation. Our ability to accurately model pinch x-ray generation for future, higher current accelerators is therefore clearly limited. On the other hand, for similar current rise times, initial pinch radii and implosion velocities to Z experiments, it is plausible that the pinch dynamics and hence pulse duration will be similar for larger drivers. This possibility is consistent with our 2D radiation MHD calculations with perturbations similar to those chosen to match Z x-ray output pulse widths. The z-pinch load used for simulations of our ICF concept consists of multiple concentric shells. The initial configuration has 2 inner shells extending from  $0.330\text{cm} < r < 0.348\text{cm}$ , and  $0.400\text{cm} < r < 0.418\text{cm}$  at density  $0.8\text{ g/cc}$ , and a distributed outer shell between  $0.418\text{cm} < r < 1.110\text{cm}$  at average density  $0.0147\text{g/cc}$  and is shown in Fig (2). Employing a Z-like current rise time of 100ns and current peak of  $\sim 63\text{ MA}$ , we have simulated a variety of initial density perturbations with results given in table I. The current and x-ray output power for the case with 10% density perturbation are shown in Fig. (3)

The more efficient emission found for an unstable pinch appears due to the conversion of additional magnetic energy through the degrees of freedom added by the instability, and by convection of the stagnating plasma that brings hot plasma to the pinch surface where it can radiate more effectively. The increased implosion velocity of plasma

in the bubbles is also advantageous for x-ray production. Fig. (4) shows development of the instability for the case with 10% random density perturbation. The simulations employ low atomic number pinch constituents (LiD) to minimize radiation trapping within the pinch observed in 1D simulations. We speculate that higher Z pinches will also radiate effectively due to the convective effect.

It is illustrative to compare the calculation with Z data for concentric wire arrays. The Z experiment, shot 227, was hydrodynamically similar to the load depicted in Fig. (2), although at an order of magnitude less mass with all of the mass concentrated in arrays of comparable mass at 0.5 cm and 1 cm radii. We expect the mass for a matched load to vary as  $I^2$  for the same radius and drive time, so a factor of  $\sim (20/60)^2 = 0.11$  is reasonable. Fig. (5) shows the signal from an x-ray detector sensitive to  $\sim 250$  eV photons. Note that the contrast, pulse shape and time between x-ray bursts are comparable.

In earlier experiments, we tested z-pinch configurations with up to four separate, concentric shells. It was found that the variation between 1D calculations, 2D calculations and experiment was considerably reduced in comparison with single shell pinches, i.e., multi-shell pinches are more calculable than a single shell pinch. This result is understandable in that the additional shells reduce instability, or at least limit the magnitude of non-linear growth of bubbles and spikes. The multi-shell pinches also tend to avoid the radiative collapse found in 1D simulations of single shells.

### III. HOHLRAUM ENERGETICS AND SYMMETRY

On Z, hohlraum temperatures of 145 eV have been obtained<sup>3</sup>. We have modeled a Z hohlraum with radius of 1.2 cm and length of 1 cm with a 2 mm power feed gap using

Lasnex<sup>8</sup>. The pinch is modeled as a planckian radiation source of fixed 2 mm diameter with a gaussian pulse of width 6 ns and peak power 129 TW, based on bare pinch (not enclosed within a hohlraum) experiments. The power and resulting hohlraum temperature, averaged over a small volume near the mid-point of the outer wall, are shown in Fig. (6). The early time discrepancy is due to neglect of the early pinch radiation not included in the gaussian pulse model.

For a wall loss dominated hohlraum, i.e., assuming the power feed gap can be kept small, and assuming the pulse duration remains the same, the radiation temperature scales as  $T \sim (E/A)^{0.3}$ , where  $E$  is the energy release and  $A$  is the wall area<sup>4</sup>. If  $E$  varies as  $I^2$ , then  $T \sim I^{0.6}$ , giving hohlraum temperatures of 280 eV at the 60 MA level for the same size hohlraum as fielded on Z, i.e. 1.2 cm radius and 1 cm length. Power feed inter-electrode gaps as small as 1.5 mm have been successfully employed, admitting a peak electrical power of 40 TW with pulse duration of 100 ns. The power feed provides a substantial sink for hohlraum x-rays, so it is critical to maintain a small gap to reach high hohlraum temperatures. It appears that the magnetic pressure ( $\sim 0.6$  MB on Z) plays a role in preventing plasma closure, an effect that we also observe in simulations at higher current. Coupling to a secondary hohlraum containing a capsule will lower the temperature due to transport inefficiencies and increasing the total wall area. We have used an analytic hohlraum model developed by M. Rosen<sup>7</sup> to evaluate the energy requirements for our ICF concept. The model is based on power balance between an x-ray source and loss to the hohlraum walls, apertures (such as the power feed) and the capsule. For a multiple hohlraum geometry, the radiation flow through the aperture linking two hohlraums is also included in the energy



sources and sinks. For a given hohlraum, labeled by index  $i$ , the energy balance model gives

$$E_{iX-ray} = E_{iWall} + E_{iHole} + E_{iCap} + E_{ij}$$

$$E_{iWall} = 0.0052 T_i^{3.3} \tau^{0.62} A_i = 0.01 T_i^4 \tau A_i (1 - \alpha_i)$$

$$E_{iHole} = 0.01 T_i^4 \tau A_{iHole}$$

$$E_{iCap} = 0.01 T_i^4 \tau A_{iCap} (1 - \alpha_{Cap})$$

$$E_{ij} = 0.01 (T_i^4 - T_j^4) \tau A_{ij}$$

Where all energies are in MJ, time,  $\tau$ , is in ns, temperature,  $T$ , is in hundred eV units (HeV) and areas are in  $\text{cm}^2$ .  $A_{iWall}$  is the wall area of the  $i$ th hohlraum and  $A_{iHole}$  is the sum of aperture areas in the hohlraum wall that do not couple to a neighboring hohlraum.  $A_{ij}$  is the area of inter-hohlraum openings, corrected for transparency in the case where a spoke array fills the opening.  $A_{ij}$  and  $A_{iHole}$  may also be corrected for hohlraum view factor effects. The albedo,  $\alpha$ , is based on gold opacity and specific heat. For alternate materials, the wall loss energy scales approximately as  $(\text{opacity})^{-0.39}$ . For instance, a gold-gadolinium hohlraum has an opacity  $\sim 1.5 \times$  gold opacity in the temperature range of 2-3 HeV, so wall losses are reduced by a factor of 0.85. We assume a gold-gadolinium hohlraum for the analytic scaling. The capsule is taken as having a fixed albedo of  $\alpha_{cap} = 0.3$  based on 1D capsule implosion modeling. For our analytic scaling, we model the system as 9 coupled hohlraums (3 in each A-K gap, 2 primary and one secondary hohlraum). X-ray sources, assumed to be of 8 ns duration are placed in the primary hohlraums with a capsule of radius 0.26 cm in the secondary hohlraum. The nominal design geometry has

1.25 cm radius primary hohlraums, 1 cm in length with 2 mm wide power feed slots on each end of a 1.6 cm long, 1 cm radius central secondary hohlraum. The power feed slots are 4 mm long. A fixed spoke array transparency of 0.75 was assumed and the shine shield radius was taken as 0.45 cm. As we vary the drive energy, the primary and secondary temperatures change as well as the capsule absorbed energy. At each drive energy, we solve the energy balance equations for the  $T_i$  values by iteration. Fig. (7) shows the resulting curves for temperature and capsule absorbed energy. The model predicts 1 MJ absorbed by the capsule and 214 eV secondary hohlraum temperature at a driver energy of 16.2 MJ.

We also find detailed calculations with Lasnex predict secondary temperatures of 210 eV or greater for 16 MJ of x-ray energy release. Fig.(8b) shows the result of a 2 dimensional hohlraum calculation with the nominal design geometry described above. The pinch is modeled as a planckian x-ray source, at time-varying radius determined from a 1D pinch calculation and with emitted energy as shown in Fig.(8a), scaled from a 1D calculation to a total yield of 16 MJ. The peak power is 2360 TW. The primary and secondary hohlraums, with 50%-50% gold-gadolinium walls to minimize wall losses, are separated by shine shields 400 $\mu$ m thick, 0.45 cm in radius and a radial spoke array extending between the shine shield and the hohlraum wall.

Efficient transmission through the spoke array separating the primary and secondary hohlraums is clearly critical. 2D radiation MHD calculations, treating the spokes as a periodic array of parallel, current-carrying rods exposed to the pinch magnetic field and hohlraum x-ray environment predict adequate transmission for 2 different spoke array designs. A 21-spoke array of 960 $\mu$ m diameter, 0.88 g/cc lithium deuteride rods gave transparency  $\sim$  50% during the foot of the pulse, rising to near 100% at the peak of the drive. A

9 spoke array of 500 $\mu$ m diameter gold rods gives more nearly constant transmission in the range 70-90%. The hohlraum calculation shown in Fig. (8) links to the gold spoke calculation for the time-dependent transmission and absorption of the spoke array, shown in Fig. (9). Fig. (10) shows the density and magnetic flux contours for the gold spoke calculation. Significant self-pinching of the gold spokes occurs in the simulation.

We can use the analytic hohlraum model to investigate sensitivity to spoke transparency. Fig. (11) shows the variation of driver energy required to provide 1 MJ absorbed capsule energy, as a function of spoke transparency. The required driver energy depends only weakly on transparency as long as the transparency exceeds 60%. Recent Z experiments, including a shot with hydrodynamically-scaled gold-loaded foam spokes at 2 g/cc, give qualitative evidence that the spoke array functions as required without degrading pinch performance. Subsequent experiments will employ a secondary hohlraum for quantitative measure of radiation transport.

We have also done 3D view factor calculations to explore the effects of pinch asymmetries, time dependent wall albedo and the non-axisymmetric perturbations due to the spoke array. Large, few millimeter scale spatial fluctuations in the pinch x-ray emission are found to have negligible effect on x-ray flux uniformity at the capsule, even if the fluctuations are assigned random 3D directions for preferential shine. Time-dependent, axisymmetric calculations with variable wall albedo and neglecting the spoke array gave time-averaged symmetry for  $P_2$ ,  $P_4$  and higher Legendre moments at the capsule less than 2%, as required for a symmetric implosion. For the time-dependent case, the shine shield radius and central hohlraum length were chosen as in the design described in section II. The greatest sensitivity is to  $P_1$  caused by power imbalances between the pinches. Left-

right power balance to 7% or better is required to remain below 2% flux asymmetry.

Static 3D calculations with a 24 spoke array showed negligible flux perturbation at the capsule, and analogous calculations for 8, 500 $\mu$ m diameter spokes showed 2% flux asymmetry.

#### IV. CAPSULE DESIGN

We have designed a capsule driven by the z-pinch driven hohlraum, shown in Fig. (12), with a Be ablator and a cryogenic fuel layer containing 3.6 mg of DT. Driven with a pulse shape similar to that shown in Fig. (8) with a peak drive temperature of 210 eV, the capsule absorbs 1MJ and yields 400 MJ in 1D simulations. We have evaluated stability against RT modes through a series of 2D calculations. We find the most unstable mode during the capsule implosion is Legendre mode  $l \sim 60$  with growth factor of 400. At ignition, the dominant mode fed through to the hot spot has  $l \sim 20$  with growth factor 350. These growth factors are similar to those found for the NIF point design<sup>4</sup>. At comparable surface roughness of a few hundred Angstroms, these capsules should have similar or slightly less converged shell distortion than the NIF point design, since the converged capsule dimensions are  $\sim$  a factor of 2 larger than for NIF. The capsule ignites with a remaining implosion kinetic energy of about 30% of the peak kinetic energy. We have also evaluated a capsule that absorbs 2MJ with drive times and capsule radii scaled by a factor of 1.26 at similar peak temperature. The 2MJ capsule has a 1D yield of 1200 MJ and readily fits within the hohlraum used to drive the 1MJ capsule. Capsule scaling arguments<sup>4</sup> indicate that a 2MJ capsule design should be possible at slightly lower drive temperature and power than at 1 MJ, although at comparable driver energy.

## V. CONCLUSIONS

We have made a preliminary evaluation of a z-pinch driven hohlraum inertial fusion concept, based on 2D radiation magnetohydrodynamic simulations and Z experiments. The nominal target configuration employs two primary z pinch driven hohlraums of the same scale as currently employed in Z experiments, with a central, secondary hohlraum linked to the primary hohlraums and containing a 5.2 mm diameter capsule. Hohlraum energetics and capsule calculations indicate that about 16 MJ of x-ray energy release, with of order 2000 TW of drive power will be required to provide 1 MJ of capsule absorbed energy. To produce the required x-ray drive and pulse shape, the pinch mass is distributed radially so as to generate pulses of the correct timing and magnitude. Simulations indicate this could be possible with accelerators that provide  $\sim 63$  MA with 100 ns rise time.

We have identified a number of critical target issues for the concept: pinch x-ray production and pulse shaping, hohlraum energetics, capsule performance and stability, spoke transparency and symmetry. Our first cut analysis of the critical issues indicates that the concept is promising. Other areas which must also be addressed, but were not discussed here, concern the pulsed power device that drives the target. These include power flow to the load and energetic photons produced in the power feeds that could lead to capsule preheat.

## ACKNOWLEDGEMENTS

The authors acknowledge useful discussions with John Nuckolls and M. Keith Matzen. This work was performed under the auspices of the U.S. Department of energy by Lawrence Livermore National Laboratory under Contract No. W-7405-ENG-48.

## REFERENCES

- <sup>1</sup>M.K. Matzen., Phys. Plasmas, 4,1519, (1997).
- <sup>2</sup>J.H. Hammer, et.al., Bull. Am. Phys. Soc., 42 , 2053, (1998).
- <sup>3</sup>J.L. Porter, Bull. Am. Phys. Soc., 42, 1948, (1998).
- <sup>4</sup>J.D. Lindl, Phys. Plasmas 2, 3933, (1995).
- <sup>5</sup>J.H. Hammer, J.L. Eddleman, P.T. Springer, M. Tabak, A. Toor, K.L. Wong, G.B. Zimmerman, C.Deeney, R. Humphreys, T.J. Nash, T.W.L. Sanford, R.B. Spielman, and J.S. DeGroot, Phys. Plasmas, 3, 2063, (1996).
- <sup>6</sup>D.L. Peterson, et.al., Phys. Plasmas, 3, 368, (1996).
- <sup>7</sup>M. Rosen, Phys. Plasmas, 3, 1803, (1996).
- <sup>8</sup>G.B. Zimmerman and W.L. Kruer, Comments on Plasma Physics and Controlled Fusion, 2, 51, (1975).

## FIGURE CAPTIONS

1. Z-pinch-driven hohlraum ICF concept
2. Z-pinch initial configuration

3. The current (a) in MA and x-ray output power(b) in TW versus time in ns, for the case with 10% density perturbation.
4. Density at different times during the implosion for the case with 10% density perturbation. The color bar at the end indicates density in g/cc.
5. X-ray detector signal (arbitrary units) vs. time (ns) for Z shot 227.
6. Calculated(blue) and experimental(green) radiation temperatures in eV, and the power used in the model (red) in TW for a Z vacuum hohlraum.
7. a) shows the primary(dashed) and secondary(solid) hohlraum temperatures versus x-ray drive energy in MJ for the analytic scaling. b) shows the capsule absorbed energy in MJ versus x-ray drive energy in MJ for the analytic scaling.
8. a) the integrated energy release of the source used to drive the 2D calculation b) radiation temperature (eV) vs. time (ns) for the 2D calculation.
9. Spoke array transmission coefficient vs. time(ns) for the case of nine 500 $\mu$ m diameter gold spokes.
10. Density(color) and magnetic flux contours for a simulation of a spoke array composed of 500 $\mu$ m diameter gold rods. The simulation has reflection symmetry boundary conditions at the left and right edge of the figure, to model an infinite array with 3.6 mm interspoke gap.
11. The variation of driver energy, in MJ, required to provide 1 MJ absorbed capsule energy, as a function of spoke transparency.
12. Capsule design that ignites with 1 MJ absorbed, yielding 400 MJ.

## TABLE CAPTIONS

I. Calculation results for x-ray yield and pulse width from 2, 1 cm long z-pinches for different perturbation levels.

Table I.

Random density seed	$E_{X\text{-ray}}(\text{MJ})$	$\Delta t(\text{ns})$	$P_{\text{max}}(\text{TW})$
1%	17.5 (16)	4.5	2400
1% new seed	17.5 (16)	6.0	1800
2%	17.5 (16)	5.0	2100
10%	21 (20)	6.0	2000
1D	14 (13)	1.7	4000

Energy in () = up to capsule bang time



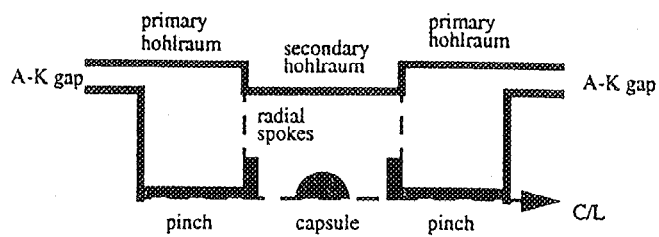


Figure 1. Hammer

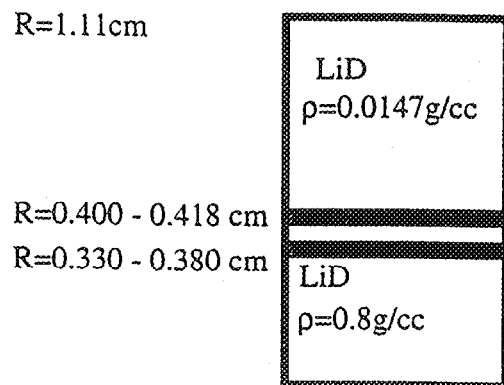


Figure 2 Hammer

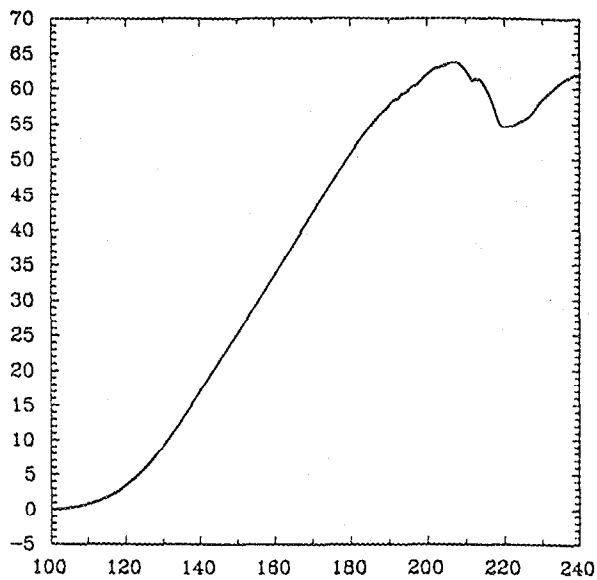


Figure 3a Hammer

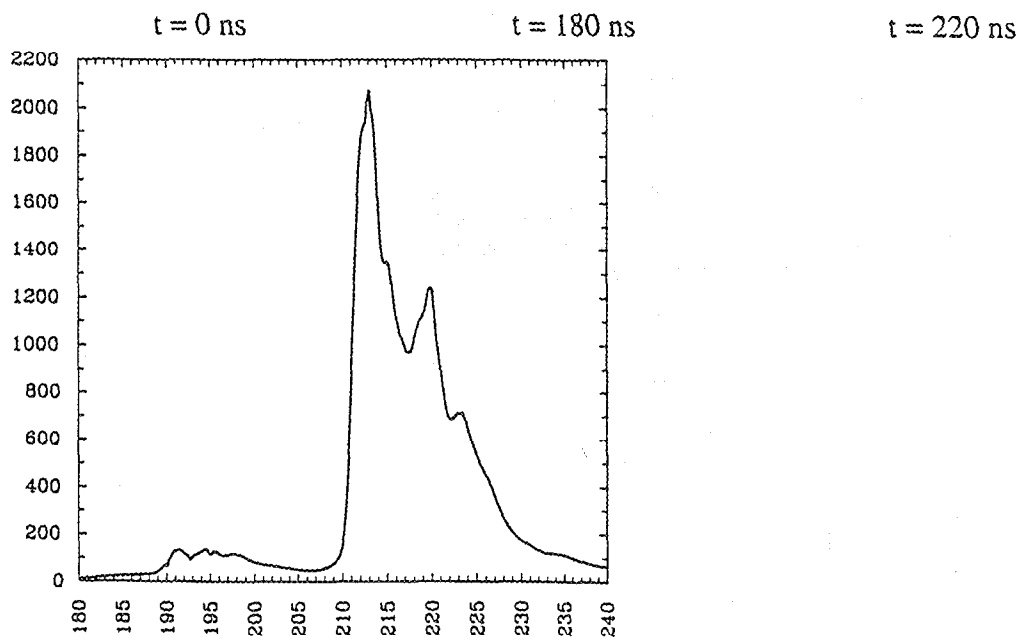


Figure 3b Hammer

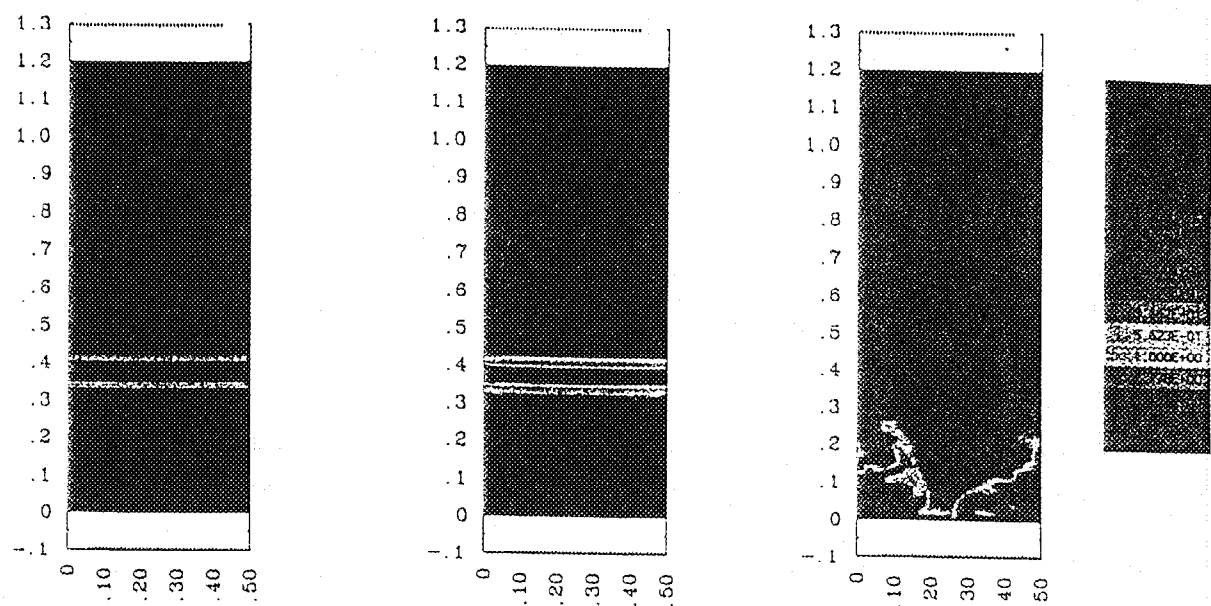


Figure 4 Hammer

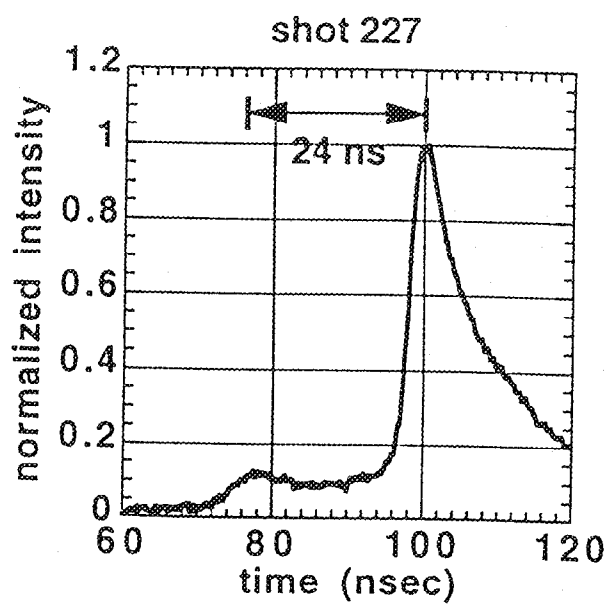


Figure 5 Hammer

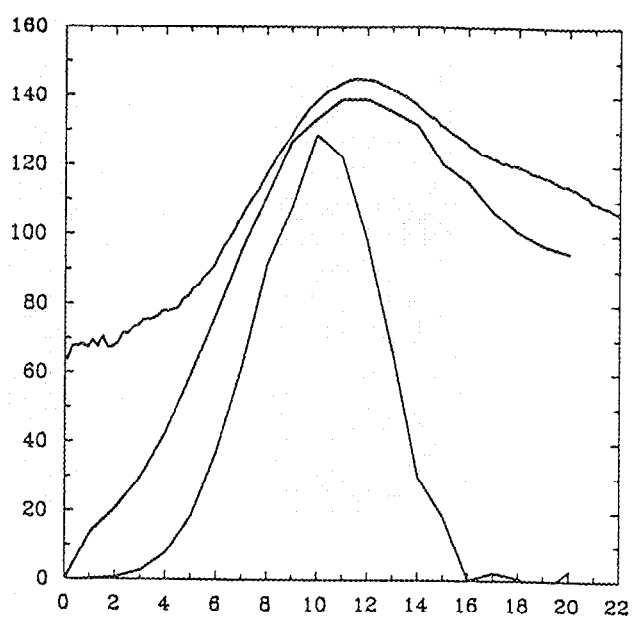


Figure 6 Hammer

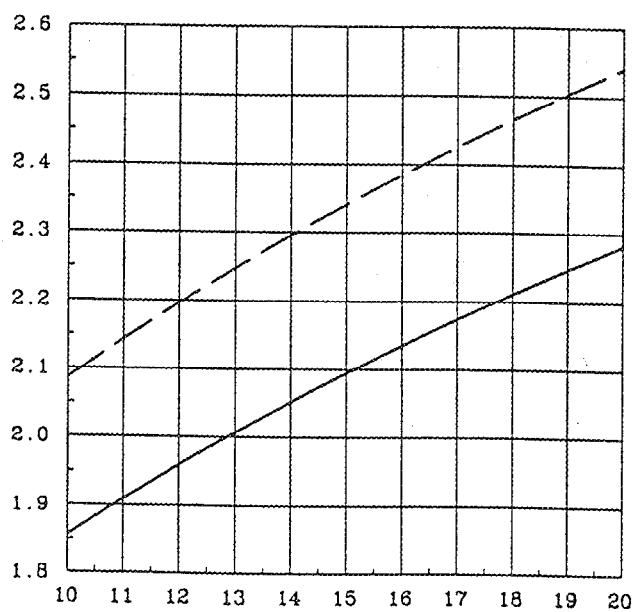


Figure 7a Hammer

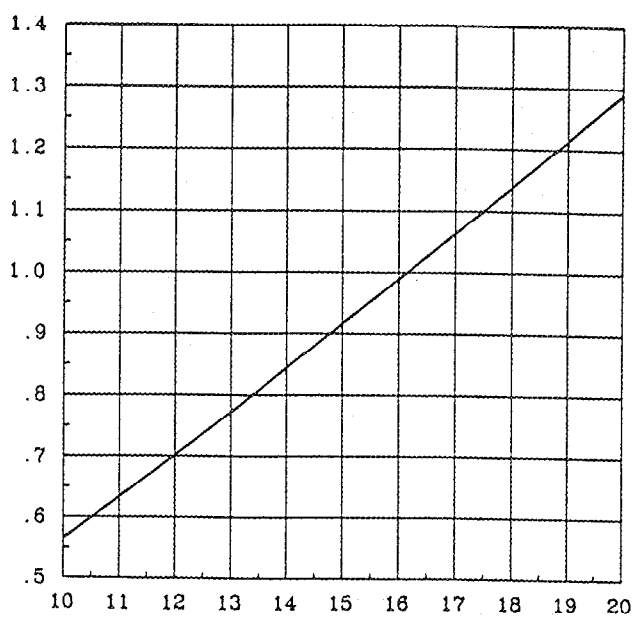


Figure 7b Hammer

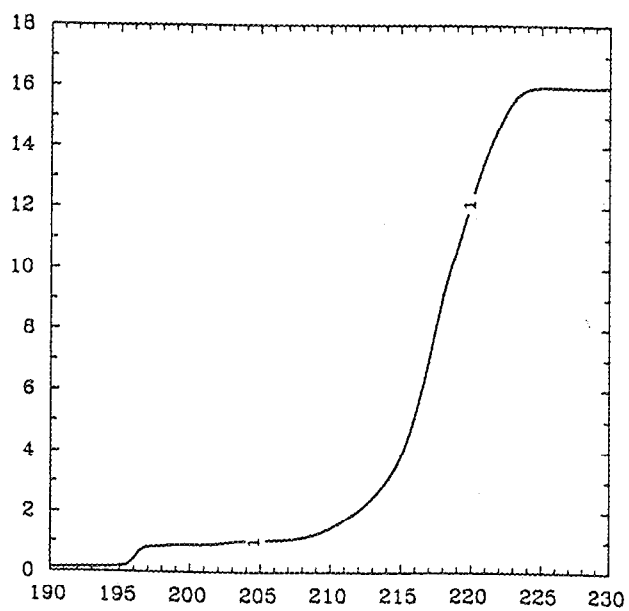


Figure 8a Hammer

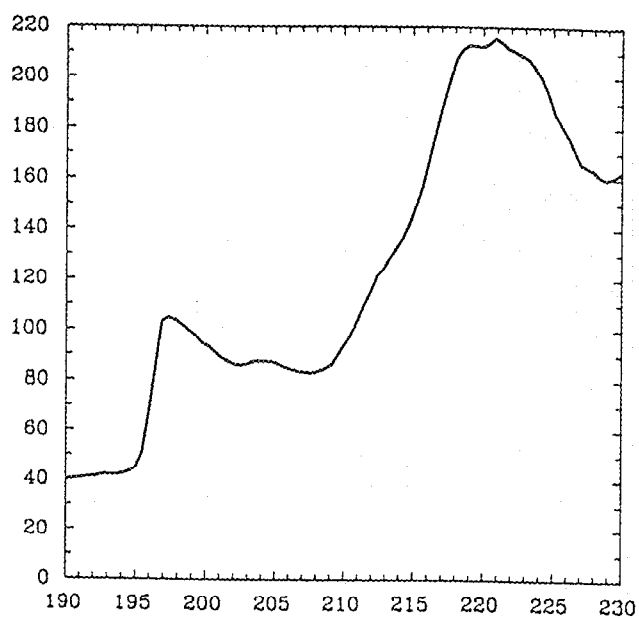


Figure 8b Hammer

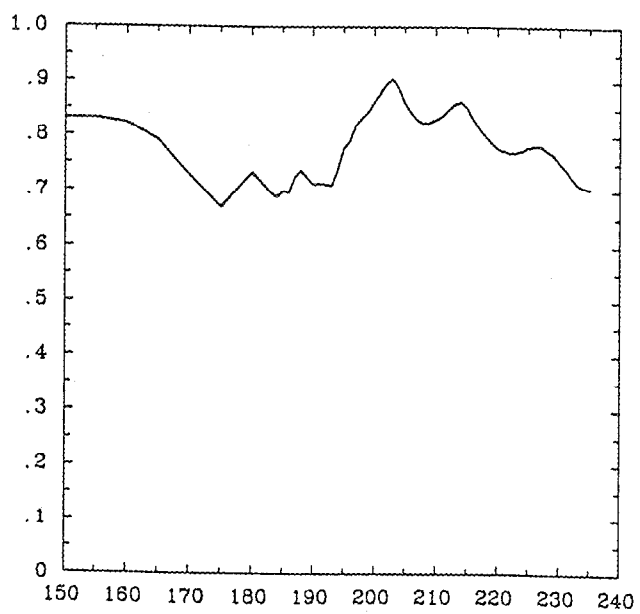


Figure 9 Hammer

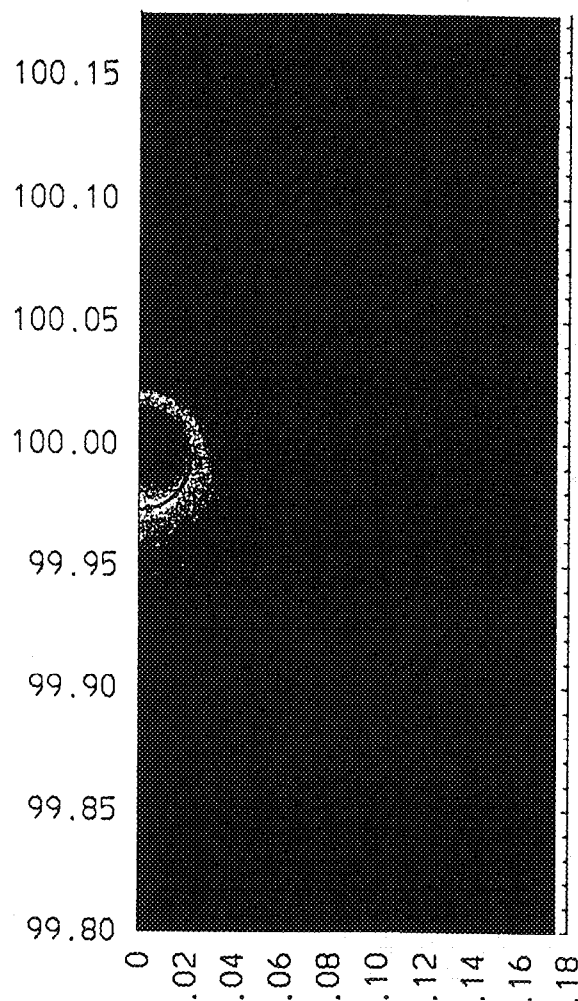


Figure 10 Hammer

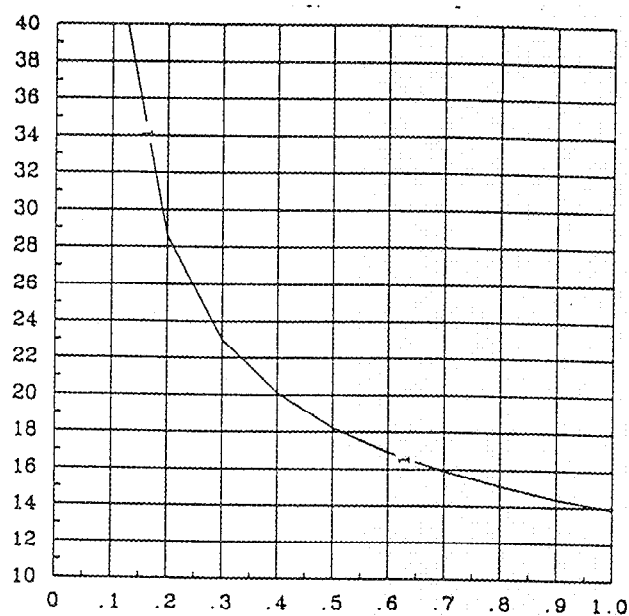


Figure 11 Hammer

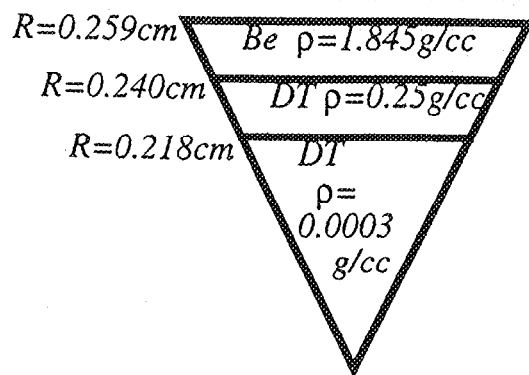


Figure 12 Hammer